HiSST: 3rd International Conference on
High-Speed Vehicle Science Technology
14 -19 April 2024, Busan, Korea

Numerical Investigation on the Flow Dynamics of Interaction between Two Liquid-liquid Bi-swirl Injectors

Vishnu Natarajan[1], Jongsu Oh[2], Jeong-Yeol Choi[3]

Abstract

In this study, numerical simulations were conducted using a validated multiphase solver implemented in OpenFOAM to investigate the flow dynamics between two bi-swirl injectors. The Volume of Fluid (VOF) method was employed to capture interface interactions, while an LES one-equation eddy viscosity model was utilized for turbulence modeling. Specifically, the study examines two distinct cases: Case-1, where both injectors swirl in the same direction, and Case-2, where they swirl in opposite directions. Our research provides a detailed exploration of the flow field, including analyses of instantaneous flow distributions, the dynamics of liquid surface waves, interracial motions between the liquids, vorticity dynamics, and the complex atomization behavior of the fuel and oxidizer. Further insights are gained by examining the plane where the sprays from the two injectors intersect. Various instantaneous flow distributions at this collision plane are studied in depth.

Keywords : *Bi-swirl Injector, Recess Length, Volume of Fluid (VOF), OpenFOAM, Atomization*

Nomenclature (Tahoma 11 pt, bold)

d – distance between injectors
L – Recess length
P – Pressure
T – Temperature
U – Velocity
α – Liquid volume fraction

1. Introduction

Within the realm of propulsion systems, the intricate dynamics of LRE injectors position them as the vital core, akin to the beating heart [1], orchestrating the combustion process in the thrust chamber. The pivotal role of injectors lies in their ability to atomize, vaporize, and seamlessly blend propellants as they traverse from the feed system to the combustion chamber, ultimately defining combustion efficiency [2]. However, the dynamic interplay of pressure oscillations within the combustion chamber can introduce fluctuations in key injector parameters—velocity, pressure, and mass flow rate—potentially unsettling the overall operational equilibrium [3]. The quest for optimal combustion efficiency underscores the need for injectors that not only facilitate thorough and uniform propellant mixing but also do so with minimal energy expenditure during atomization and mixing processes [4]. Injectors thus emerge not only as sculptors of propellant characteristics but also as architects of stability and efficiency in the broader context of LRE systems.

Swirl injectors have emerged as indispensable elements in LREs, distinguished by their proficiency in fostering efficient mixing and atomization. The inherent swirling motion instigates the outward expansion of the liquid film, generating a center toroidal recirculation zone downstream of the injector [5]. These injectors boast high flow rates, delivering superior thrust per injector element, and exhibit

[1] *Graduate Research Assistant, Pusan National University, natarajanvishnu7@gmail.com*
[2] *Graduate Research Assistant, Pusan National University, ohjong1103@naver.com*
[3] *Professor, Pusan National University, aerochoi@pusan.ac.kr*

excellent throttling capability. Notably, the larger flow passages in swirl injectors make them less susceptible to the impact of manufacturing errors. Comparative studies reveal that swirl injectors achieve mean droplet diameters 2.2-2.5 times smaller than those generated by jet injectors with equivalent pressure drops and mass flow rates [4]. Swirl injectors exhibit two distinct configurations: closed-type and open-type [6], distinguished by their geometric shapes. The bi-swirl injector is a type of swirl injector used in bi-propellant LREs where both the fuel and oxidizer are supplied through two coaxial swirl injectors.

Theoretical investigations into swirl injector dynamics date back to the 1940s [7]. Subsequent works by Bazarov and Yang [2-4] provided valuable insights, demonstrating that the overall response of a swirl injector can be comprehended by examining the transfer characteristics of its individual components. The experimental studies on bi-swirl injectors have primarily centered around exploring the impact of recess length on propellant mixing behavior and its spray characteristics. Notable experimental studies by Sivakumar and Raghunandan [8, 9]. extensively investigated the dynamics of liquid-liquid bi-swirl injectors. Their research delved into the intricate relationship between recess length and droplet size, revealing that variations in recess length adversely affected atomization. Kim et al. [10] also conducted experimental studies to investigate the influence of recess length on the spray properties of a liquid-liquid bi-swirl injector. Yoon and Ahn [11] undertook both experimental and theoretical investigations to evaluate the influence of recess length, swirl direction, and mixture ratio on the spray cone angles of a bi-swirl injector.

Numerical studies [12] were carried out to explore the flow dynamics of bi-swirl injectors under supercritical conditions. The study systematically explored various injector configurations, specifically varying the recess region, post thickness, and kerosene annulus width. Ding et al. [13] delved into a study on liquid sprays in liquid-liquid coaxial swirling jets, utilizing a LES-VOF model. The research focused on the structure and flow field of coaxial swirling jets, employing monomethyl hydrazine as fuel and mixed oxides of nitrogen as oxidizer. Lee et al. [14] performed a numerical study on bi-swirl injectors with various recess lengths. In the previous study [15], the authors conducted a numerical investigation on a bi-swirl injector using water for different recess lengths. The authors also conducted complete flow dynamics of single bi-swirl injector [16] using non-volatile oxygen and kerosene for various recess lengths. While previous studies have provided insights into individual aspects, there is a notable gap in research focusing on the intricate flow dynamics of the interaction between two bi-swirl injectors. Therefore, this study makes a concerted effort to explore the interplay in flow dynamics between two bi-swirl injectors, employing a three-dimensional multiphase flow simulation with LES for a detailed analysis.

2. Numerical methodology

Multiphase flow simulations of the bi-swirl injector are carried out using the open-source CFD software OpenFOAM. The VOF method is employed to accurately track the interfaces between different fluid surfaces in the simulation.

2.1. Governing equations

The continuity and momentum equations for the solver used are given by

$$\nabla.(\vec{U}) = 0 \tag{1}$$

$$\frac{\partial \rho \vec{U}}{\partial t} + \nabla.\left(\rho \vec{U}\vec{U}\right) = -\nabla P + \nabla.T + \rho \vec{F}_b \tag{2}$$

The phase continuity equation is

$$\frac{\partial \alpha}{\partial t} + \nabla.\left(\vec{U}\alpha\right) = 0 \tag{3}$$

where α is the volume fraction of fluid. The value of α for each fluid ranges between 0 and 1. With advancements in computational power in the recent decades, LES has risen to prominence as a compelling methodology for turbulence modeling [17]. For modeling the turbulence, LES one-equation eddy viscosity subgrid model is used in this study.

The numerical approach involves the discretization of governing equations using the finite-volume method on an unstructured grid. A second-order implicit, bounded Crank-Nicolson scheme is utilized for time integration. Gauss linear interpolation is employed to compute gradients by interpolating values from cell centers to face centers. Divergence terms are treated by means of linear interpolation except for the divergence of φ (flux across cell faces) and α, for which the van Leer limiter is employed. The corrected scheme is used for the surface normal gradient. In spite of the low non-orthogonality of the grid, 2 non-orthogonal iterations were used in the simulations to obtain a satisfactory balance between computational efficiency and solution accuracy. For LES, the zero-gradient conditions are set for nut and inletOutlet, and a uniform value of 10^{-5} is used for *k*. The smooth delta filter is used for the LES within which the delta type is cubeRootVol with deltaCoeff of 1.0 and maxDeltaRatio of 1.1. The value of Ck is 0.094. The mass and momentum conservation equations are calculated using the PISO algorithm. The pressure term is solved using a preconditioned conjugate gradient solver with the diagonal incomplete-Cholesky preconditioner, and a smooth solver with the Gauss-Seidel smoother was employed to solve all other terms. The error tolerance is set to 10^{-8} and the relative tolerance is set to 0. This means that iterations would continue until the absolute error in the solution falls below 10^{-8}. The average number of iterations for solving the pressure field is approximately 650. The present numerical approach is expected to yield reliable results for the flow physics under consideration

2.2. Injector configuration and boundary conditions

The bi-swirl injector used in this study is the injector utilized in the RD-0110 engine. In this configuration, the oxidizer is supplied via inner closed-type injector and the fuel is supplied via outer open-type injector. The bi-swirl injector, mirroring the RD-0110 engine's configuration, exhibits a total length of 24.2 mm and an exit diameter of 10 mm. The outer open-type injector spans 10.5 mm in length, featuring an outer diameter of 10 mm and a width of 1.5 mm. Cylindrical tangential inlets, each with a length of 5 mm, populate both outer and inner injectors. The diameters of these inlets measure 0.7 mm and 1.7 mm for the outer and inner injectors, respectively. Positioned at fixed distances from the center, the tangential inlets for the outer and inner injectors are located at 4.5 mm and 3.5 mm, respectively. Maintaining a recess length (L) of 5 mm between the inner and outer injectors in the bi-swirl configuration facilitates the convergence of fuel and oxidizer within the injector. The two bi-swirl injectors are positioned at a distance (d) equal to half the injector exit diameter, i.e., 5 mm, in this study.

In this study, two distinct cases are investigated as shown in Fig. 1. In Case-1, both bi-swirl injectors exhibit swirling motion in the same direction, while in Case-2, the bi-swirl injectors swirl in opposite directions. It is noteworthy that within each bi-swirl injector unit, the inner and outer injectors consistently exhibit swirling motion in the same direction. To investigate the liquid breakup characteristics and spray pattern outside the injector, an external domain was also included at the injector exit. To study the effect of liquid-liquid flow dynamics in the bi-swirl injector, LOX is considered non-volatile and it stays liquid throughout the simulation. Therefore, non-volatile LOX is considered as the oxidizer and kerosene is used as the fuel in this study. The boundary conditions used for the single bi-swirl injector [16] is used for here too.

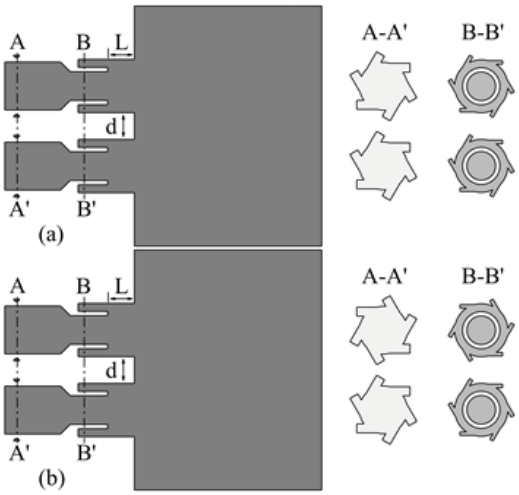

Fig 1. Schematic of the two bi-swirl injector configurations swirling in (a) same direction (Case -1) (b) opposite direction (Case -2).

The computational grid system employs an unstructured grid comprising tetrahedral cells, as depicted in Fig.2. The head of the inner injector is zoomed to show the grids in the tangential inlets. The very-fine mesh case comprises a total of 11,081,972 nodes, with cells sized between 100-200 μm throughout the computational domain. The smallest cells are primarily used in the injection orifices and near the injector walls. The larger cells are mostly for the exterior domain. The total number of cells for the very-fine mesh case is 63,246,056. The maximum Courant number is set at 0.5 to ensure numerical stability. The computational domain is divided into 1104 subdomains using the Scotch decomposition method in OpenFOAM, and the decomposed domain is then computed using MPI. The simulation is performed for a certain period of time to ensure that the flowfield develops completely and reaches a fully stationary state.

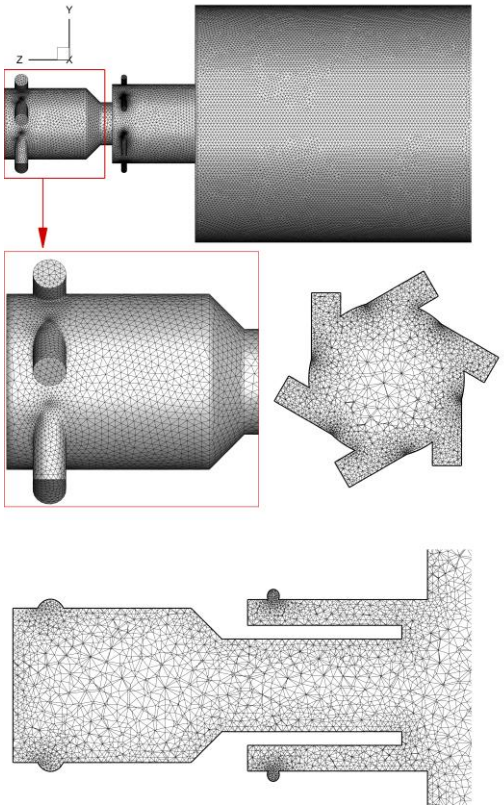

Fig 2. Computational grid and the oxidizer inlet parts zoomed in for clarity. (coarse mesh is shown for clarity)

3. Results and discussion

3.1. Instantaneous flowfield

The instantaneous volume fraction contour for the bi-swirl injector configuration with two injectors is presented in Fig. 3. In a single bi-swirl injector both the fuel and oxidizer meets within the injector. The flow interface displays a wavy pattern along the stream wise direction, indicative of fluctuations or undulations within the flow. Within the injector, a conspicuous helical flow path is observed, suggesting a swirling or spiral motion of the fluid during its passage. Moreover, an irregular and uneven variation in the thickness of the liquid film is apparent inside the injector. This non-uniformity in film thickness implies an inconsistent distribution of liquid within the injector. Measurements of film thickness and spray cone angles were conducted at various locations and times, and the averaged values, both spatially and temporally, provide meaningful insights. Specifically, the measured film thickness for the internal mixing bi-swirl injector is 0.78 mm, while the spray cone angle measures 56^0. The

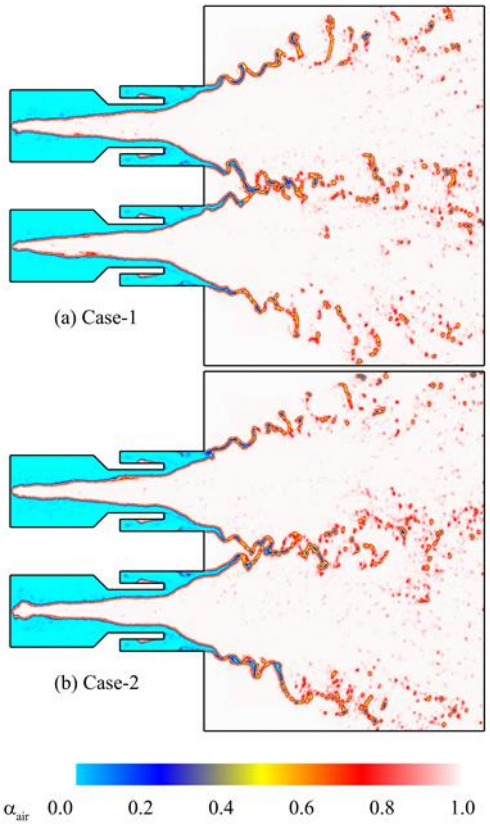

Fig 3. Air volume-fraction field showing the instantaneous flow development.

Notably, distinct air cores are evident within both the inner and outer injector flows. The direction of swirl becomes evident through the surface waves near the air core region, as illustrated in Fig. 4. The formation of an air core within the injector, coupled with the swirling motion of the liquid flow around the chamber, serves as a dampening mechanism for pressure fluctuations traveling from the combustion chamber to the feed system and vice versa. The flow from the two bi-swirl injectors meets outside the injector and forms a spray pattern. In Case-1, although the flows from both bi-swirl injectors swirl in the same direction, they collide in opposite directions at the meeting region of the sprays. This results in a strong interaction and potentially more flow disruptions due to the collision of the two flows. On the other hand, in Case-2, the flows from both injectors are in the same direction at the meeting region. This leads to a more coherent flow pattern and potentially smoother interaction, as the flows are not directly opposing each other. The unstable surface waves on the outer surface of the swirling flows is distinctly visible.

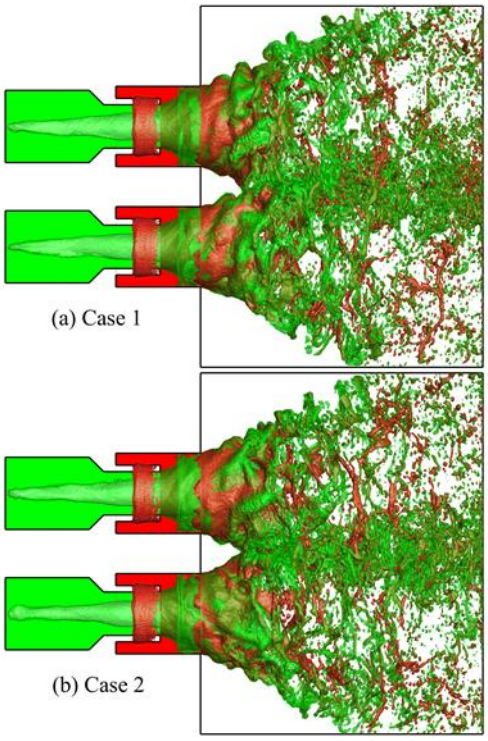

Fig 4. Instantaneous volume fraction distribution and iso-surface distribution of fuel and oxidizer. (Green color denotes oxidizer and red color denotes fuel)

Fig.4 depicts the flow field and spray characteristics resulting from the interaction of fuel and oxidizer in two configurations of a bi-swirl injector, visualized using volume fractions and iso-surface where green represents the oxidizer and red represents the fuel. The flow fields in both cases are highly complex and turbulent, which is indicated by the intricate patterns and intermingling of green and red regions. The extensive intertwining of green and red areas suggests that the mixing of the oxidizer and fuel is intense, which is a desirable feature in combustion processes. In Case-1, the interaction between the two streams appears to be more chaotic. This is attributed to the meeting of the two sprays in opposite directions, leading to increased collisions and breakup of the flow streams. Conversely, in Case-2, the flow exhibits a more coherent behavior, characterized by elongated structures due to meeting of the two sprays in the same direction.

The fuel and oxidizer are atomized as they exit the injectors, breaking into smaller droplets. The density and size distribution of droplets can be inferred from the concentration of red and green dots. High-density areas may represent regions of less efficient atomization, while the sparser areas suggest finer atomization. Notably, the liquid film surface exhibits distinct axial and azimuthal surface waves along the outer injector passage, which gradually evolve into instability waves. The ultimate breakdown of the liquid sheet occurs as it exits the injector, a point at which inertial forces surpass viscous and surface tension forces. The growth of instability waves, after exiting the injector, as the liquid spreads outwards, plays a pivotal role in initiating the liquid sheet breakup. This breakup initiates at the wave antinode, where the liquid film is relatively thin, making it more susceptible to rupture. It's important to note that the instability waves consist of both varicose and sinuous modes. The domination of the varicose mode contributes to the liquid sheet breakup, while the growth of instability waves is primarily driven by the sinuous mode.

3.2. Vorticity

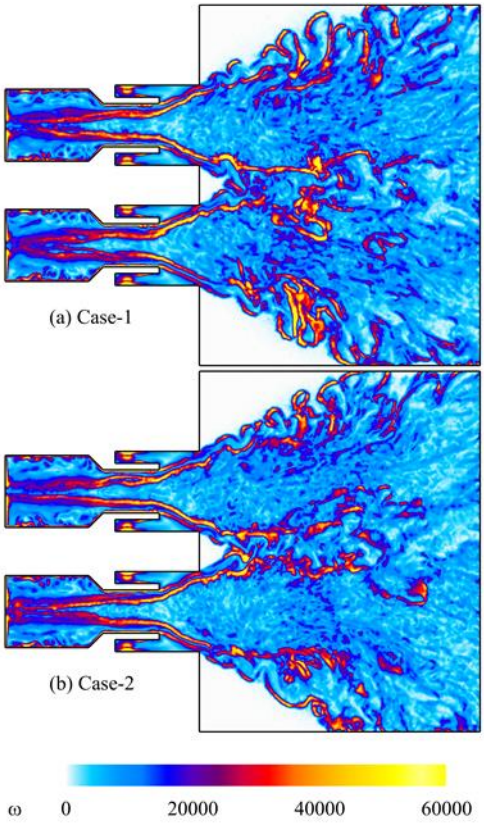

Fig 5. Instantaneous distribution of vorticity magnitude.

The distribution of vorticity magnitude is vividly depicted in Fig. 5. It's evident that the vorticity magnitude is significantly elevated along both the inner and outer surfaces of the swirling flow field, indicating the pronounced swirl motion induced by the injectors. These observations highlight the presence of elongated structures characterized by high vorticity, signifying dynamic processes such as vortex stretching. These processes are fundamental in turbulence and contribute to the energy cascade from larger to smaller scales, ultimately enhancing the efficiency and stability of combustion. In Case-1, the regions with high vorticity magnitude appear to be more elongated and concentrated, particularly in the meeting region where the two sprays collide. The notable gradient between high and low vorticity regions suggests the presence of significant shear layers, which could promote the formation of smaller-scale structures and improved mixing. However, this may also result in increased pressure loss. Conversely, in Case-2, the high vorticity areas are somewhat more dispersed, which could potentially lead to lower pressure loss compared to Case-1.

3.3. Flow dynamics at the collision plane

To gain deeper insights into the flow dynamics, we focus on the plane situated between the two bi-swirl injectors, where the sprays from both injectors collide. The flow field distributions in this collision plane are depicted in Fig. 6, revealing valuable information about the behavior of fuel, and oxidizer within this region. The volume fraction contours of air, fuel, and oxidizer illustrate how these components are distributed in the collision plane. Notably, the spray pattern is more dispersed in Case-1 compared to Case-2. Moreover, there appears to be a higher concentration of oxidizer droplets in Case-1. The amount and dispersion of droplets are clearly visible in the images. In Case-1, the collision of the two sprays results in a concentrated fluid region at the outset, and due to the intense collision, the droplets disperse rapidly. Conversely, in Case-2, both fuel and oxidizer initially spread outward, forming a network-like structure before breaking down into droplets. The vorticity distribution and the velocity vectors shows the formation of vortices within the collision plane. Strong vortices are found in the area between the liquid fuel and oxidizer. The vorticity distribution and velocity vectors provide insights into the formation of vortices within the collision plane. Strong vortices are observed in the area between the liquid fuel and oxidizer. In Case-1, the vortices appear more widespread, and they

are almost symmetrical on both sides since the flows from both injectors meet in opposite directions. In Case-2, a high vorticity region is noticeable on the left-hand side, which corresponds to the location where both sprays collide while swirling in the same direction. The direction of these vortices can be discerned by examining the distribution of velocity vectors.

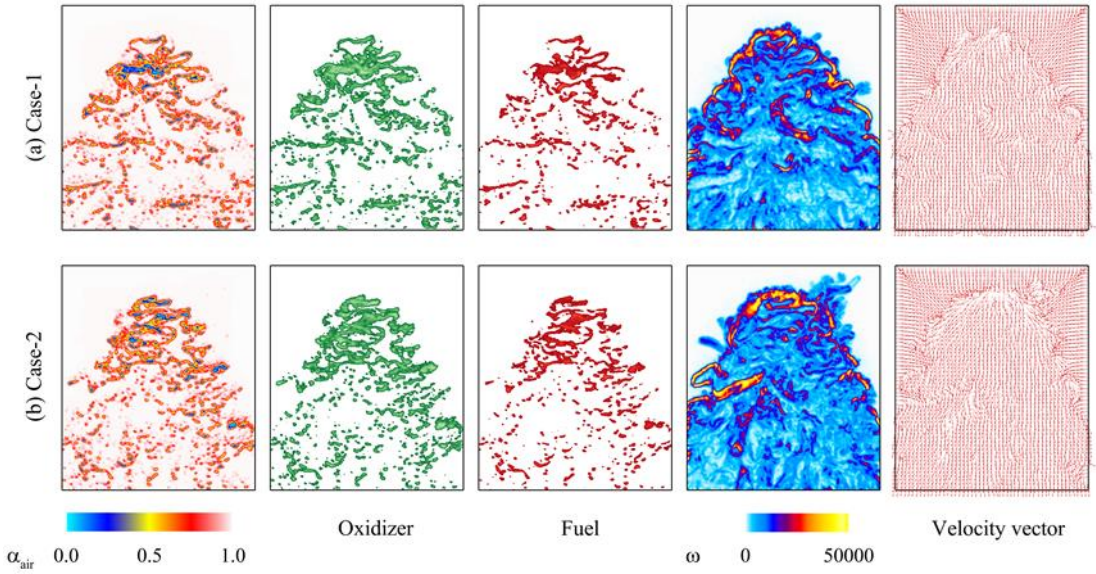

Fig 6. Various instantaneous flow field distributions at the collision plane.

4. Concluding remarks

This study presents ground-breaking advancements in understanding the flow dynamics and atomization characteristics of two interacting internal mixing bi-swirl injectors. The three-dimensional, LES multiphase flow simulations, meticulously conducted in OpenFOAM with a validated solver, have yielded pivotal insights. The robust validation of the solver, through a classical droplet impingement problem and an extensive grid refinement study, has ensured the reliability of the current research findings. The investigation of two scenarios – injectors swirling in the same direction (Case-1) and in opposite directions (Case-2) – has been instrumental in elucidating the impact of swirl direction on flow dynamics and atomization. Significantly, we observed that in Case-1, where injectors swirl in the same direction but collide oppositely, there is an increase in droplet formation. Conversely, in Case-2, the collision in same direction lead to fewer droplets

Acknowledgements

Present work was supported by the Space Launch Vehicle and Space Transportation Education and Research Center (NRF-2022M1A3C2076724) through National Research Foundation (NRF) of Korea, funded by the Ministry of Science and ICT (MSIT) of the Republic of Korea Government.

References

1. R. W. Humble, H. N. Gary, and W. J. J. Larson, "Space propulsion analysis and design," (1995).
2. V. Bazarov, Influence of propellant injector stationary and dynamic parameters on high frequency combustion stability (AIAA 1996-3119, 1996).
3. V. G. Bazarov, and V. Yang, "Liquid-propellant rocket engine injector dynamics," Journal of Propulsion and Power 14, 797 (1998).
4. V. Bazarov, V. Yang, and P. Puri, Design and dynamics of jet and swirl Injectors (American Institute of Aeronautics and Astronautics, 2004).
5. X. Wang, H. Huo, Y. Wang, and V. Yang, "Comprehensive study of cryogenic fluid dynamics of swirl injectors at supercritical conditions," AIAA Journal 55, 3109 (2017).
6. V. Natarajan, U. Unnikrishnan, W.-S. Hwang, J.-Y. Choi, and V. Yang, "Numerical study of

two-phase flow dynamics and atomization in an open-type liquid swirl injector," International Journal of Multiphase Flow 143, 103702 (2021).
7. G. N. Abramovich, The theory of swirl atomizers (Moscow, Russia, 1944).
8. D. Sivakumar, and B. N. Raghunandan, "Hysteretic interaction of conical liquid sheets from coaxial atomizers: Influence on the spray characteristics," Physics of Fluids 10, 1384 (1998).
9. D. Sivakumar, and B. N. Raghunandan, "Formation and separation of merged liquid sheets developed from the mixing of coaxial swirling liquid sheets," Physics of Fluids 15, 3443 (2003).
10. D. Kim, P. Han, J.-H. Im, Y. Yoon, and V. G. Bazarov, "Effect of Recess on the Spray Characteristics of Liquid-Liquid Swirl Coaxial Injectors," Journal of Propulsion and Power 23, 1194 (2007).
11. W. Yoon, and K. Ahn, "Experimental and Theoretical Study on Spray Angles of Bi-Swirl Coaxial Injectors," journal of Applied Fluid Mechanics 11, 1377 (2018).
12. X. Wang, Y. Wang, and V. Yang, "Geometric effects on liquid oxygen/kerosene bi-swirl injector flow dynamics at supercritical conditions," AIAA Journal 55, 3467 (2017).
13. J.-W. Ding, G.-X. Li, and Y.-S. Yu, "Numerical investigation on liquid sheets interaction characteristics of liquid-liquid coaxial swirling jets in bipropellant thruster," International Journal of Heat and Fluid Flow 62, 129 (2016).
14. B. Lee, W. Yoon, Y. Yoon, and K. Ahn, "Numerical Study on Swirl Coaxial Injectors with Different Recess Lengths," Journal of ILASS-Korea 23, 49 (2018).
15. V. Natarajan, W.-S. Hwang, B.-K. Sung, and J. Choi, Two-phase flow study of the RD-0110 engine injector with different recess lengths (American Institute of Aeronautics and Astronautics, 2021).
16. V. Natarajan, U. Unnikrishnan, J.-Y. Choi, and V. Yang, "Flow dynamics of a liquid–liquid bi-swirl injector," Physics of Fluids 36, (2024).
17. A. Balabel, "Numerical modeling of turbulence-induced interfacial instability in two-phase flow with moving interface," Applied Mathematical Modelling 36, 3593 (2012).